ELSEVIER

Journal of Photochemistry and Photobiology A: Chemistry 156 (2003) 207–218

Journal of Photochemistry and Photobiology A:Chemistry

www.elsevier.com/locate/jphotochem

Photophysics and photocatalytic properties of Ag^+-activated sandwich Q-CdS–TiO_2

Anil Kumar*, Arvind Kumar Jain

Department of Chemistry, Indian Institute of Technology Roorkee, Roorkee 247667, India

Received 2 May 2002; received in revised form 8 October 2002; accepted 12 October 2002

Dedicated to Prof. P. Natarajan on his 60th birthday

Abstract

The photophysical and photocatalytic behavior of sandwich $Cd(OH)_2$-coated Q-CdS–Ag_2S and the mixture of sandwich colloidal semiconductors consisting of Ag^+-containing Q-CdS–TiO_2 and Ag^+-doped TiO_2–$Cd(OH)_2$-coated Q-CdS have been examined. The addition of Ag^+ to $Cd(OH)_2$-coated Q-CdS causes the quenching of bandgap emission of CdS and induces simultaneously the red emission. For a typical $[Ag^+]$ (2.0×10^{-5} mol dm^{-3}) the average lifetime ($\langle\tau\rangle$) of $Cd(OH)_2$-coated Q-CdS decreases from 19.97 to 15.99 ns whereas at 650 nm it increases from 7.72 to 14.68 ns. Unlike stoichiometric Q-CdS–Ag_2S system these particles do not sensitize the reaction of indole–O_2 redox couple. Coupling of Ag^+-containing $Cd(OH)_2$-coated Q-CdS with TiO_2 as well as of Ag^+-containing TiO_2 with $Cd(OH)_2$-coated Q-CdS quenches the 462 nm emission of CdS completely and produces a new emission band at around 650 nm. Quenching of emission fits to a Perrin model. In both the cases the doping of Ag^+ modifies the TiO_2 phase. At high $[Ag^+]$ it produces a three component composite catalyst, CdS–TiO_2–Ag_2S. The photogenerated hole CdS (h^+) in the Ag^+-activated composite CdS–TiO_2 catalyst forms an emissive exciplex with indole and results in its decomposition to yield indigo. The photoinduced charge separation in this system was twofold higher compared to the undoped composite photocatalyst (CdS–TiO_2). This catalytic action of Ag^+ is understood in terms of the positive redox potential of the Ag^+/Ag couple, which serves to intercept the conduction band electron and reduces the e^-–h^+ recombination.

Keywords: Photophysics; Photocatalytic; Photooxidation of indole; Q-CdS–Ag_2S; Ag^+-activated Q-CdS–TiO_2; Q-CdS–TiO_2–Ag_2S

1. Introduction

Heterogeneous photocatalysis initiated by colloidal semiconductors has drawn considerable attention over the last one decade in view of their large specific surface, high redox potential of the photogenerated charge carriers and selective reduction and oxidation of different class of organics at their interface [1–6]. The utilization of solar energy to effect these processes requires using the low bandgap material as a sensitizer. The photochemical efficiency of the reactions studied at their interface is often poor as the majority of the charge carriers recombine readily through radiative or non-radiative pathways. Besides, the high recombination rate of e^-–h^+ pair compared to the rate of electron transfer to the oxygen, being used generally as an electron acceptor, further limits the efficiency of this system [1]. An improvement in their catalytic activity necessitates increasing the charge separation in the illuminated photocatalyst by enhancing the lifetime of the e^- and h^+. An elegant approach to meet these requirements is to make use of coupled photocatalyst [5–12] in which the small bandgap component is used as sensitizer and the large bandgap component having low energy of conduction band acts as a sink for photogenerated electron. It would thus separate the two charge carriers effectively. The coupled catalysts have not been examined as yet extensively for performing synthetic photochemical reactions. In our recent study we have employed $Cd(OH)_2$-coated Q-CdS–TiO_2 composite catalyst [12] for the photooxidation of indole. $Cd(OH)_2$-coated Q-CdS did not induce its photochemical reaction but its coupling with TiO_2 initiated this reaction efficiently and produced indigo with a quantum efficiency of 0.08.

Addition of metal/metal ion to a semiconductor is known to affect their both photophysical behavior as well as photochemical reactivity [2,13–15]. Metals affect the surface properties by generating a Schottky barrier of the metal in contact with semiconductor's surface, which acts as an electron trap. Similarly, the addition of transition metal ions to semiconductors improves the trapping of electron

---

* Corresponding author. Tel.: +91-1332-85799; fax: +91-1332-73560.
E-mail address: anilkfcy@iitr.ernet.in (A. Kumar).

1010-6030/03/$ – see front matter © 2003 Elsevier Science B.V. All rights reserved.
PII: S1010-6030(02)00396-9

and inhibits e^-–h^+ recombination. In the present work we have investigated the effect of addition of metal ions on the photoactivity of the composite photocatalyst (CdS–TiO_2). Interestingly, the addition of Ag^+ to each of its component prior to their coupling activates this photocatalyst and at high [Ag^+] it leads to the generation of hitherto unreported three components system (CdS–TiO_2–Ag_2S). The photocatalytic activity of this sensitizer is increased by about twofold compared to the sandwich CdS–TiO_2 catalyst. The photophysics and photocatalytic properties of these particles have been examined by addition of Ag^+ to each of the components of the catalyst prior to and after their coupling. Indoles have been found to be among several effluents present in the industrial coal waste [16].

2. Experimental

2.1. Materials

All chemicals used in the present study were of analytical grade. Cadmium perchlorate (Alfa); indole, indigo (Aldrich); sodium hexametaphosphate (Qualigens); silica gel G, chloroform, carbon tetrachloride, sodium hydroxide, perchloric acid, silver nitrate (E. Merck) were used as received. Titanium tetrachloride (Reidel de Häen) was distilled under vacuum. The dialysis membrane was spectra/por with mw cut-off 6000–8000.

2.2. Equipment

Electronic spectra were recorded on Shimadzu UV-2100 S and DU-6 Beckman spectrophotometers. Emission spectra were measured on a Shimadzu RF-5301-PC spectrofluorophotometer. Steady-state photolysis was carried out on an Oriel photolysis assembly equipped with 200 W Hg (Xe) arc lamp, solution and glass cut filters. Electron microscopy was performed by a Philips CM-10 transmission electron microscope equipped with a 35 mm camera by applying an accelerating voltage of 100 kV. The fluorescence lifetimes were measured on an IBH-5000 single photon counting fluorimeter using a picosecond Ti-sapphire mode locked laser for excitation. Hamamatsu photomultiplier was used for detection of fluorescence. Decay curves were analyzed by iterative reconvolution technique. The multiexponential fitting program was provided from IBH.

2.3. Methodology

Colloidal CdS [17] and colloidal TiO_2 [18] particles were synthesized by following the earlier methods except SH^- was injected to precipitate CdS. Cadmium hydroxide was coated on CdS particles by adding excess of NaOH followed by excess Cd^{2+} ($\geq 6 \times 10^{-4}$ mol dm^{-3}) to the stoichiometric 3×10^{-4} mol dm^{-3} CdS particles. The pH of this solution was maintained at 11.0. Colloidal TiO_2 particles were synthesized by slow addition of $TiCl_4$ to water at 0 °C. Thus prepared colloidal CdS and TiO_2 were spherical in shape having an average size of 6 and 8 nm, respectively. Colloidal CdS was activated with different amounts of Ag^+ by its quick addition under vigorous shaking. Silver-doped TiO_2 was prepared by addition of Ag^+ to the ice cold water prior to the addition of $TiCl_4$. This solution was subsequently dialyzed at about 5 °C till pH lay around 3. The coupling of Ag^+-containing CdS with TiO_2 and Ag^+-doped TiO_2 with CdS was carried out by quick injection of TiO_2/TiO_2–Ag^+ to CdS–Ag^+/CdS solutions, respectively. The interaction between CdS and TiO_2 in these mixed colloids was checked by monitoring the photophysics of CdS and recording their electron micrographs (Fig. 1). TEM pictures clearly reveal the coupled particles to be aggregated which formed bigger clusters unlike naked $Cd(OH)_2$-coated Q-CdS. Actinometry was performed using a ferrioxalate actinometer. The product(s) of reaction was identified by TLC and its amount was estimated spectrophotometrically.

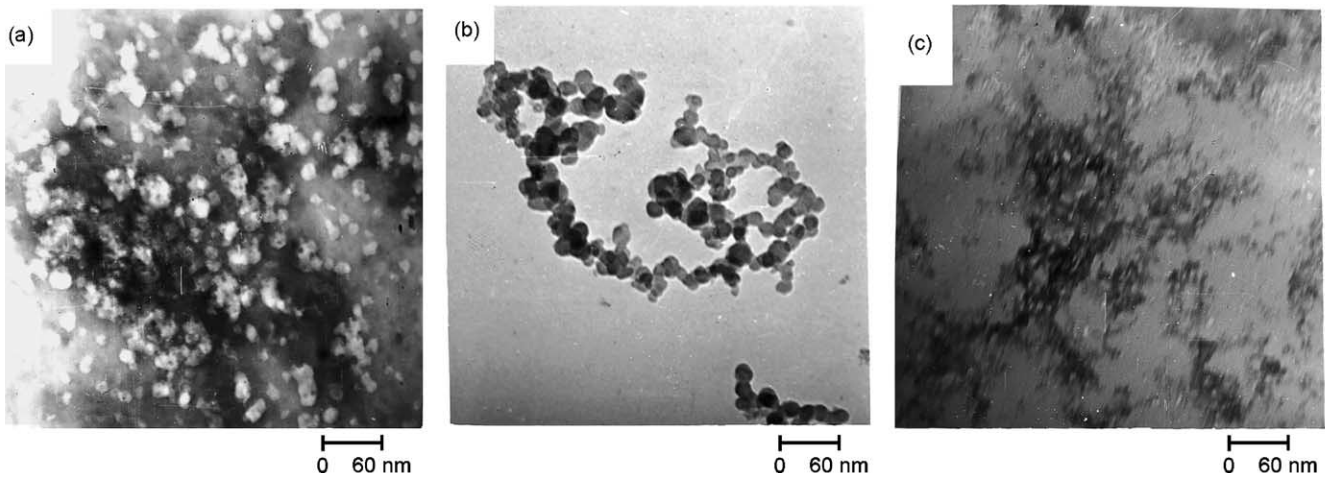

Fig. 1. TEM micrograph of: (a) $Cd(OH)_2$-coated Q-CdS, (b) $Cd(OH)_2$-coated Q-CdS–TiO_2, (c) $Cd(OH)_2$-coated Q-CdS coupled with Ag^+-doped TiO_2.

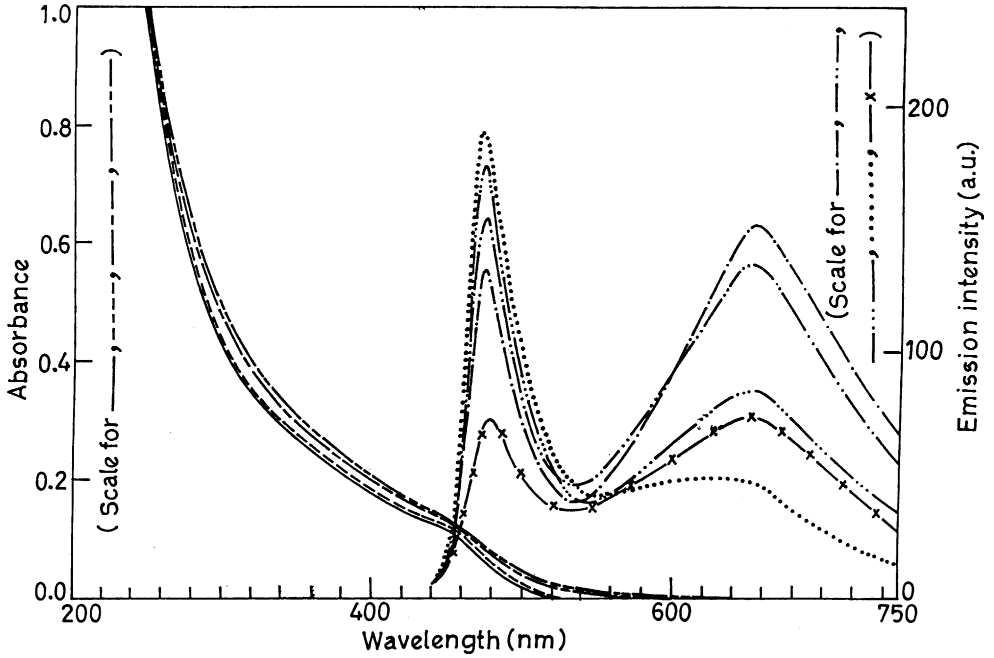

Fig. 2. Electronic spectra of $Cd(OH)_2$-coated Q-CdS (1.35×10^{-4} mol dm^{-3}) containing [Ag^+] ($\times 10^{-5}$ mol dm^{-3}): 0.0 (—); 0.5 (- - -); 2.0 (– – –); 3.0 (– - - -). Emission spectra of $Cd(OH)_2$-coated Q-CdS doped with different [Ag^+] ($\times 10^{-5}$ mol dm^{-3}): 0.0 (···); 0.5 (–····–); 1.0 (–···–); 2.0 (–·–); 4.0 (–×–), $\lambda_{ex} = 400$ nm.

3. Results and discussion

3.1. *Effect of activation by silver on photophysical and photocatalytic properties of $Cd(OH)_2$-coated Q-CdS*

The electronic and emission spectra of $Cd(OH)_2$-coated Q-CdS before and after activating with different amounts of silver are shown in Fig. 2. At low [Ag^+] ($<3.5 \times 10^{-6}$ mol dm^{-3}) the absorption spectrum of Q-CdS remains unaffected but at its higher concentrations ($\geq 4 \times 10^{-6}$ mol dm^{-3}) the absorption threshold gets red shifted. For a typical 3×10^{-5} mol dm^{-3} of Ag^+ the bandgap shifts from 2.36 to 1.97 eV.

In emission spectroscopy the addition of Ag^+ to the Q-CdS causes the quenching of its excitonic emission weakly and simultaneously develops a new band at around 650 nm at its higher concentrations ($\geq 4 \times 10^{-6}$ mol dm^{-3}). The intensity of the 650 nm band was found to enhance with an increase in Ag^+ up to 2×10^{-5} mol dm^{-3} and thereafter it starts decreasing. The above observations suggest that Ag^+ at its low concentrations ($<3.5 \times 10^{-6}$ mol dm^{-3}) remains dissolved in the CdS lattice [15] due to which the electronic and emission spectra are not affected. The addition of higher amounts of silver generates anion vacancies at the interface of $Cd(OH)_2$-coated Q-CdS which induces the red emission. At high concentrations of silver a separate Ag_2S phase is produced which though lowers the bandgap of the sandwich CdS–Ag_2S catalyst but does not participate in the enhancement of emission. This argument is also supported by the fact that pure Ag_2S does not exhibit any emission in the recorded wavelength region.[1]

To analyze the dynamics of the charge carriers in this system the emission lifetime of $Cd(OH)_2$-coated Q-CdS was monitored both in the absence and presence of different amounts of silver at 462 nm as well as 650 nm. A few representative fluorescence decay curves at these wavelengths are shown in Fig. 3. All decay curves were found to be the best-fit into a three-exponential program. From these traces the average lifetime ($\langle\tau\rangle$) of the charge carriers was evaluated using Jame's equation [19]. Tables 1 and 2 present the kinetic analysis of different components of decay curve at 462 and 650 nm. The activation of $Cd(OH)_2$-coated Q-CdS with a typical 2×10^{-5} mol dm^{-3} Ag^+ reduces the average fluorescence lifetime at 462 nm from 19.97 to 15.99 ns whereas at 650 nm the $\langle\tau\rangle$ is increased from 7.73 to 14.68 ns. The bandgap emission of $Cd(OH)_2$-coated Q-CdS (462 nm) has been considered to be the excitonic emission [20–22] arising due to the trapping of one of the charge carriers in the shallow trap and the 650 nm band has been attributed due to the recombination of trapped e^-–h^+ [23,24]. A slight decrease in the fluorescence lifetime of bandgap emission can be understood by the interception of conduction band electron present in shallow traps by Ag^+. The enhancement of lifetime of red emission may be attributed to the increased trapping of e^- and h^+ pair in deep traps in the presence of Ag^+.

---

[1] In a separate experiment colloidal Ag_2S was synthesized by injecting SH^- to $AgNO_3$ solution using sodium hexametaphosphate as stabilizer.

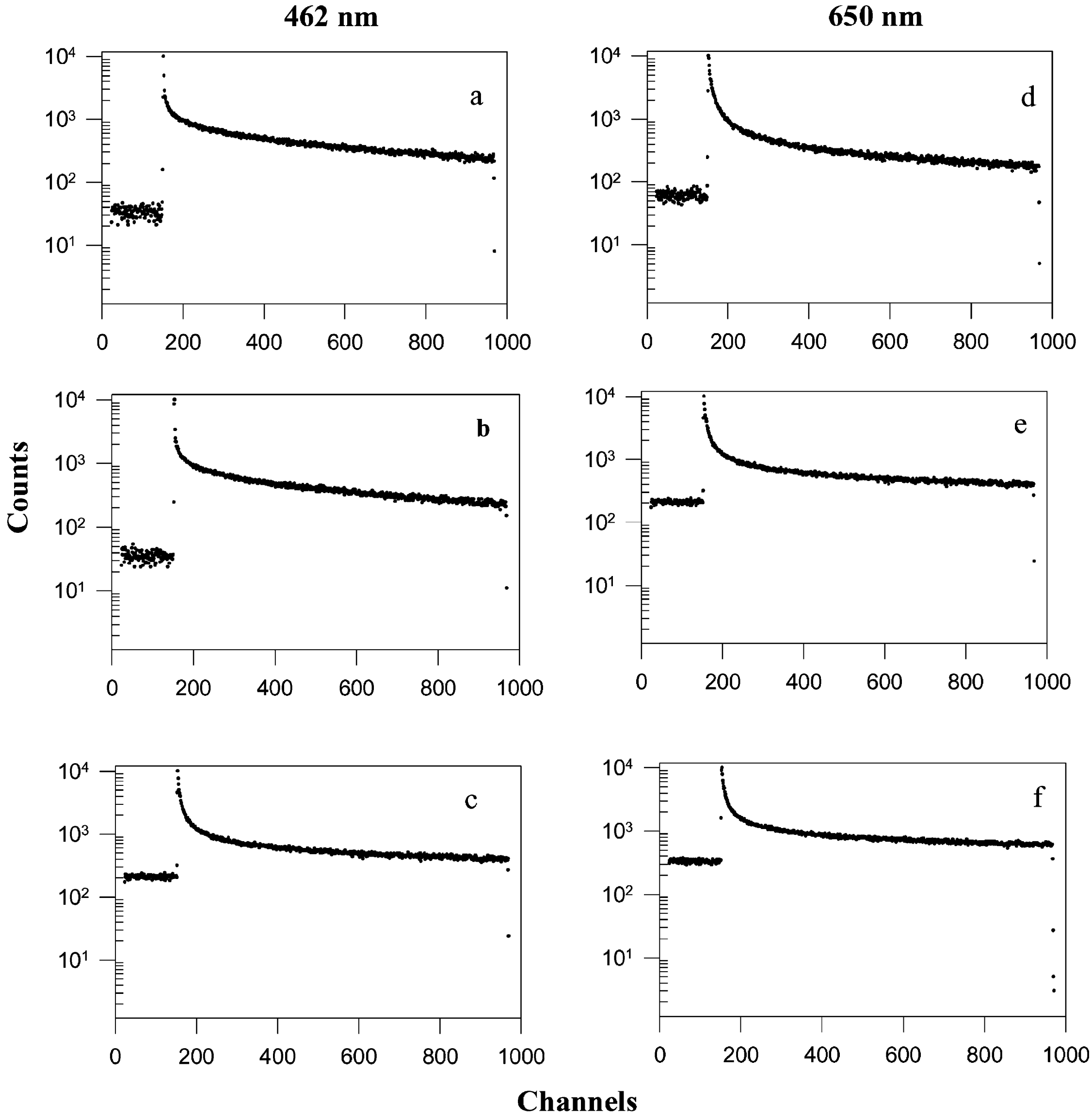

Fig. 3. Fluorescence decay curves for $Cd(OH)_2$-coated Q-CdS in the presence of different amount of $[Ag^+]$ ($\times 10^{-5}$ mol dm^{-3}) at 462 and 650 nm: 0.0 (a, d); 1.0 (b, e); 2.0 (c, f) at $\lambda_{ex} = 440$ nm. Time calibration: 5.079×10^{-11} s/channel.

Table 1
Emission lifetime measurements at 462 nm[a]

$Cd(OH)_2$-coated Q-CdS (1.35×10^{-4} mol dm^{-3})	Component 1		Component 2		Component 3		$\langle\tau\rangle$ (ns)	χ^2
	τ_1 (ns)	Emission (%)	τ_2 (ns)	Emission (%)	τ_3 (ns)	Emission (%)		
Pure	0.44 (5.38)	2.84	3.37 (3.04)	12.39	23.06 (3.04)	84.77	19.97	0.998
Containing Ag^+ (1.0×10^{-5} mol dm^{-3})	0.45 (45.86)	2.18	2.68 (37.45)	10.52	18.74 (44.44)	87.30	16.65	1.018
Containing Ag^+ (2.0×10^{-5} mol dm^{-3})	0.30 (5.55)	2.13	2.04 (3.79)	9.87	17.94 (3.84)	88.00	15.99	1.059
Coupled with pure TiO_2	0.34 (0.13)	15.27	2.00 (4.28E−2)	30.53	7.19 (0.02)	54.19	4.46	1.115
Coupled with TiO_2 doped with Ag^+ (3.5×10^{-7} mol dm^{-3})	0.29 (0.14)	12.91	1.59 (0.05)	25.28	6.27 (3.12 E−02)	61.81	4.32	1.207

[a] Values given in the bracket denote the pre-exponential factor corresponding to the respective τ.

Table 2
Emission lifetime measurements at 650 nm[a]

$Cd(OH)_2$-coated Q-CdS (1.35×10^{-4} mol dm^{-3})	Component 1		Component 2		Component 3		$\langle\tau\rangle$ (ns)	χ^2
	τ_1 (ns)	Emission (%)	τ_2 (ns)	Emission (%)	τ_3 (ns)	Emission (%)		
Pure	0.40 (16.25)	13.13	1.77 (6.79)	24.03	11.54 (2.71)	62.83	7.73	1.075
Containing Ag^+ (1.0×10^{-5} mol dm^{-3})	0.30 (148.72)	6.01	1.61 (94.48)	20.27	12.56 (43.98)	73.72	9.61	1.042
Containing Ag^+ (2.0×10^{-5} mol dm^{-3})	0.41 (157.62)	5.62	2.40 (87.08)	18.26	18.68 (46.64)	76.12	14.68	1.020
Coupled with TiO_2	0.40 (0.38)	7.54	2.06 (0.17)	16.74	17.14 (0.09)	75.72	13.31	1.071
Coupled with Ag^+ (3.5×10^{-7} mol dm^{-3}) doped TiO_2	0.47 (0.34)	5.36	2.90 (0.13)	12.81	26.91 (8.95E−02)	81.83	22.40	1.512

[a] Values given in the bracket denote the pre-exponential factor corresponding to the respective τ.

These particles were fairly photostable and underwent photodissolution with a quantum efficiency of <0.002 similar to that of non-activated $Cd(OH)_2$-coated Q-CdS. To check their photocatalytic activity these particles were used to sensitize the reaction of indole–O_2 redox couple. In the presence of indole–O_2 redox couple the photophysics of $Cd(OH)_2$-coated Q-CdS activated with silver remains unaffected. The illumination of this catalyst by light of $\lambda >$ 400 nm, where indole does not possess any absorption, did not initiate any appreciable reaction of indole ($\phi_{\text{indole}} <$ 0.002). It was also revealed by the absence of any product of its oxidation. This behavior is different to that of stoichiometric Ag^+-activated CdS in which the separation of charge and the redox reactivity are enhanced [15]. Thus in the presence of silver the e^- and h^+ pair remain trapped at the interface of the CdS in relatively deep traps which undergo radiative recombination and enhance the red emission but still cannot escape the surface of Q-CdS particles coated by $Cd(OH)_2$ layer to scavenge O_2 and indole, respectively. This can be explained by the low solubility product of cadmium hydroxide compared to that of silver hydroxide [25,26].

3.2. Electronic properties of coupled $Cd(OH)_2$-coated Q-CdS–TiO_2 activated with Ag^+

3.2.1. Optical behavior

In these experiments one of the component of the composite catalyst ($Cd(OH)_2$-coated Q-CdS/TiO_2) was activated with Ag^+ prior to their coupling with another component. The absorption spectra of Ag^+-containing $Cd(OH)_2$-coated Q-CdS before and after coupling with TiO_2 are shown in Fig. 4. The coupling of the two shifts the excitonic peak of CdS to higher energy from 450 to 420 nm and exhibits slight change in the absorption spectra. At low [Ag^+] ($<3.5 \times 10^{-6}$ mol dm^{-3}) the absorption threshold of the coupled semiconductors was not very different to the non-activated CdS–TiO_2 but at higher [Ag^+] ($>4 \times 10^{-6}$ mol dm^{-3}) it shifts to the red. The low [Ag^+] ($<3.5 \times 10^{-6}$ mol dm^{-3}) corresponds to about 2% equivalent of CdS and at this concentration a large amount of Ag^+ is known to remain dissolved in the CdS lattice [15,27,28]. Similar electronic spectral changes were observed upon coupling of Ag^+-doped TiO_2 with $Cd(OH)_2$-coated Q-CdS at high [Ag^+]. However, relatively much less [Ag^+] were used for doping of the TiO_2 phase compared to those added to CdS phase and under these conditions no change in optical absorption was noted (inset, Fig. 4).

3.2.2. Emission behavior

Coupling of Ag^+-containing $Cd(OH)_2$-coated Q-CdS with TiO_2 quenches the bandgap emission of CdS completely even at the lowest used [Ag^+] (3.5×10^{-6} mol dm^{-3}) (Fig. 5a). At low [Ag^+] ($<3.5 \times 10^{-6}$ mol dm^{-3}) the red emission band was not affected, however, at higher [Ag^+] ($>4 \times 10^{-6}$ mol dm^{-3}) the 650 nm band simply grows without causing any spectral shift up to 3×10^{-5} mol dm^{-3} of Ag^+. Thereafter, the intensity of this band decreases. Similar observations were recorded upon coupling of $Cd(OH)_2$-coated Q-CdS with Ag^+-doped TiO_2. The addition of Ag^+-doped TiO_2 to the colloidal $Cd(OH)_2$-coated Q-CdS causes the quenching of its bandgap emission along with a simultaneous enhancement of red emission (Fig. 5b). The enhancement of red emission in this case is similar to those when Ag^+-containing CdS was coupled with TiO_2 except that increase in emission intensity was of a little less magnitude. These data do not fit to a simple Stern–Volmer equation and demonstrate a curvature at high concentrations of Ag^+-doped TiO_2 (Fig. 6a). On the other hand, Perrin model depicts relatively a better fit (Fig. 6b). From this curve an effective quenching volume of donor–acceptor (Q-CdS–Ag^+-doped TiO_2) quenching sphere is calculated to be 4.03×10^3 Å^3. The fact that emission intensity data do not fit well to a Stern–Volmer relationship suggests the absence of diffusion of Ag^+-doped TiO_2 to excited CdS to demonstrate a bimolecular quenching. On the other hand, a better fitting of emission data to a Perrin Model indicates the donor and acceptor to be associated to form such a cluster which is unable to change its spatial position with respect to each other during the process of quenching. A fairly large value of quenching sphere suggests the electron transfer from the excited CdS to TiO_2 to be more facile and this is indeed the case (Fig. 6b). The above observations also indicate that Ag^+ remains dissolved at its low concentration in the CdS lattice but at higher concentrations, a

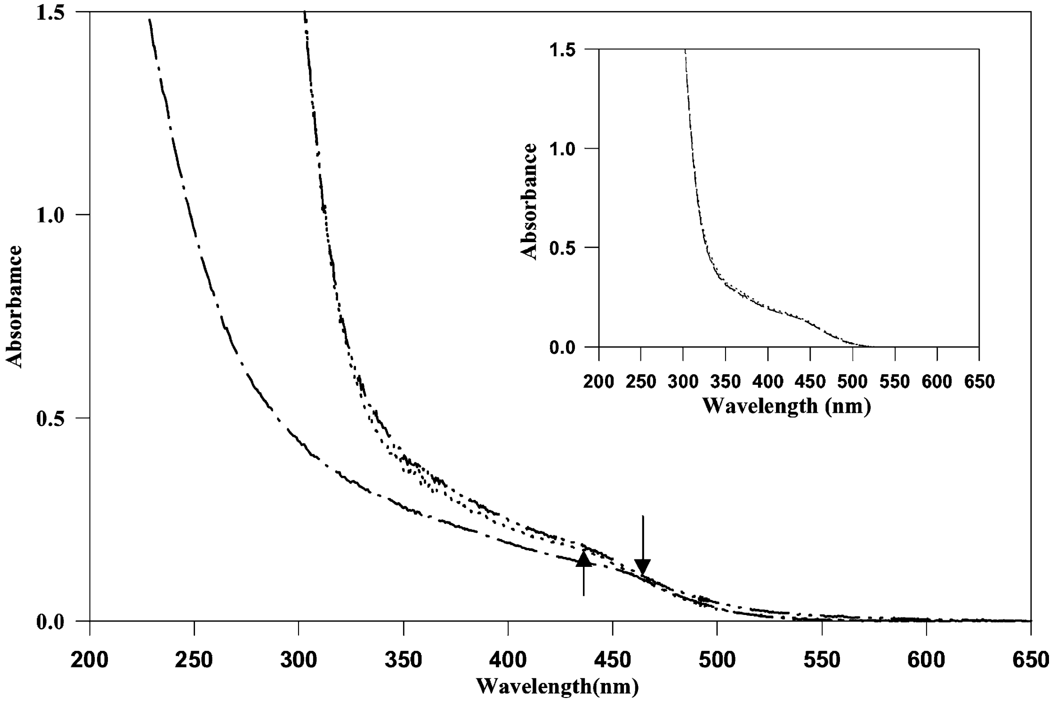

Fig. 4. Electronic spectra of Ag^+-activated $Cd(OH)_2$-coated Q-CdS before (–·–) and after coupling with TiO_2 (1.28×10^{-3} mol dm^{-3}) containing different amounts of Ag^+ ($\times 10^{-5}$ mol dm^{-3}) in CdS phase: 1.0 (···) and 3.0 (–· –). Inset: electronic spectra of $Cd(OH)_2$-coated Q-CdS (1.35×10^{-4} mol dm^{-3}) coupled with TiO_2 doped with [Ag^+] ($\times 10^{-7}$ mol dm^{-3}): 0.0 (––) and 1.75 (···).

separate Ag_2S phase is precipitated which does not emit in the red region (see footnote 1). This composite photocatalyst thus consists of three components TiO_2, CdS and Ag_2S phases (CdS–TiO_2–Ag_2S).

3.2.3. *Photodecomposition*

The decomposition of CdS phase for different oxygenated catalysts activated with Ag^+ viz. Q-CdS–Ag_2S, Ag^+-containing $Cd(OH)_2$-coated Q-CdS coupled with TiO_2 and Ag^+-doped TiO_2 coupled with $Cd(OH)_2$-coated Q-CdS as a function of illumination time by light of $\lambda > 400$ nm are shown in Fig. 7. The highest decomposition is observed when TiO_2 component is doped with Ag^+ and then coupled to $Cd(OH)_2$-coated Q-CdS. Obviously, TiO_2-doped with Ag^+ modifies this phase so as to enhance the trapping of more e^- as shown below (Eqs. (1)–(4)) and thus hole can oxidize more of CdS.

$$Cd(OH)_2 \cdot CdS \xrightarrow{h\nu} Cd(OH)_2 \cdot CdS(e^-–h^+) \tag{1}$$

$$Cd(OH)_2 \cdot CdS(e^-) + TiO_2 \rightarrow CdS + TiO_2(e^-) + Cd^{2+} + 2OH^- \tag{2}$$

$$TiO_2(e^-) + Ag^+ \rightarrow TiO_2 + Ag \tag{3}$$

$$TiO_2(e^-) + O_2 \rightarrow TiO_2 + O_2{}^- \tag{4}$$

$$CdS(h^+) + CdS + O_2 + O_2{}^- \rightarrow Cd^{2+} + SO_4{}^{2-} + CdS \tag{5}$$

3.2.4. *Charge dynamics*

Relaxation of charge carriers in the composite catalyst (CdS–TiO_2) without and with Ag^+ in TiO_2 phase were followed by monitoring the decay of emission at 462 and 650 nm (Fig. 8). These samples were illuminated by light of 375 nm, which is absorbed by CdS phase only as colloidal TiO_2 does not have any absorption at this wavelength. All these traces depicted multiexponential decay and were found to be the best-fit in three-exponential program. Tables 1 and 2 present the kinetic analysis of decay curves at 462 and 650 nm. At 462 nm $\langle\tau\rangle$ reduces from 4.46 to 4.32 ns, whereas at 650 nm $\langle\tau\rangle$ is increased from 13.31 to 22.40 ns. Interestingly, at 650 nm amongst three lifetime components it is the third component which has relatively a longer time constant and high percentage emission, and arises due to radiative recombination of the trapped charge carriers. It is this long time constant component which contributes predominantly to the increased average lifetime at 650 nm in the presence of Ag^+. These observations indicate an increased transport of shallowly trapped electron from the conduction band of CdS to the TiO_2 phase and trapping of more charge carriers into the deeper traps in the presence of Ag^+.

3.2.5. *Photophysics and photocatalytic activity of Ag^+-activated $Cd(OH)_2$-coated Q-CdS–TiO_2 system in the presence of indole–O_2 couple*

In order to check the separation of charge in the illuminated composite catalyst, its photophysics and photocatalytic activity were monitored in the presence of indole–O_2

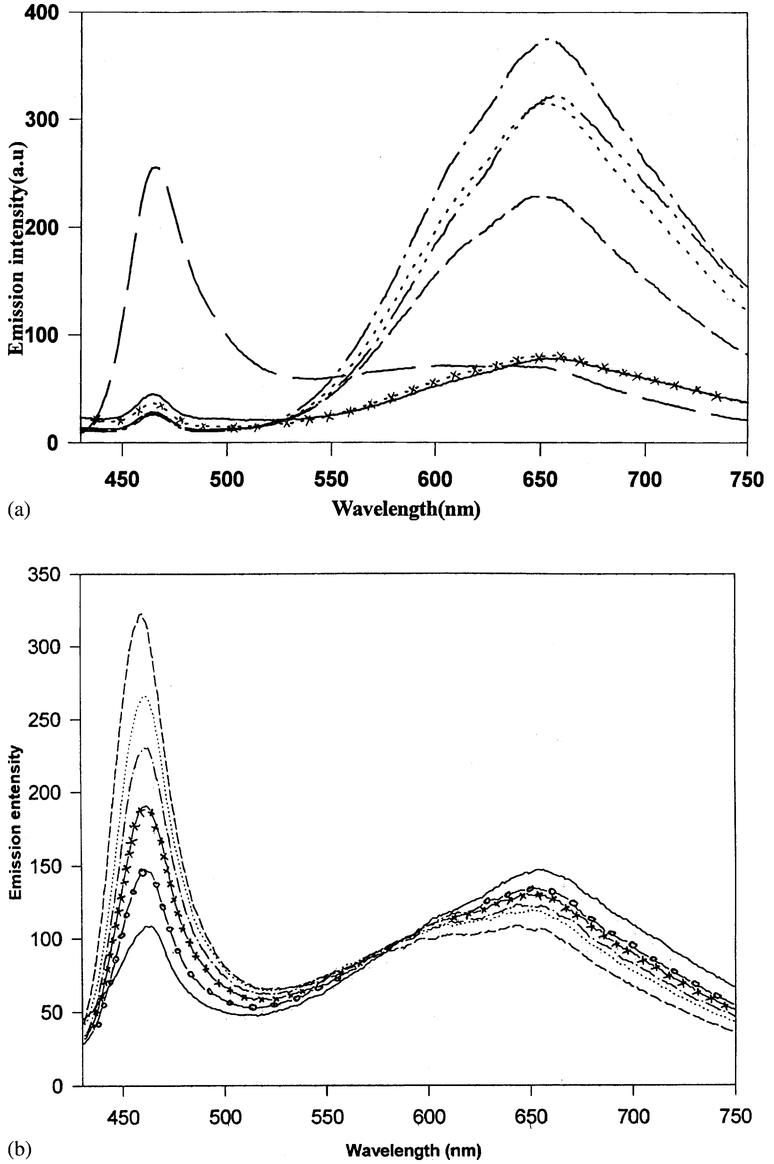

Fig. 5. (a) Emission spectra of pure Cd(OH)$_2$-coated Q-CdS (——) and Cd(OH)$_2$-coated Q-CdS doped with different amounts of Ag$^+$ before coupling with TiO$_2$ (1.28×10^{-3} mol dm^{-3}) [Ag$^+$] ($\times 10^{-5}$ mol dm^{-3}): 0.35 (–×–); 1.0 (–––); 2.0 (···); 3.0 (–·–), 4.0 (–···–) at pH = 11.0. Emission spectrum of Cd(OH)$_2$-coated Q-CdS (1.35×10^{-4} mol dm^{-3}) coupled with TiO$_2$ (1.28×10^{-3} mol dm^{-3}) doped with Ag$^+$ (3.5×10^{-7} mol dm^{-3}) (—), $\lambda_{ex} = 400$ nm. (b) Emission spectra of Cd(OH)$_2$-coated Q-CdS in the presence of different [Ag$^+$ (3.5×10^{-7} mol dm^{-3})-doped TiO$_2$] ($\times 10^{-4}$ mol dm^{-3}): 0.0 (---); 1.46 (···); 1.83 (–·–); 2.20 (–×–); 2.56 (–○–); 3.30 (—).

redox couple. In these experiments each of the CdS and TiO$_2$ component was activated with Ag$^+$ prior to their coupling with other non-activated component. In the first case Ag$^+$ was added to Q-CdS solution prior to its coupling with TiO$_2$. The excitation of this catalyst in the presence of indole by light of $\lambda \geq 400$ nm where indole does not have any absorption causes the production of a new fluorescence band at around 495 nm. The intensity of this band was found to depend on [indole] (Fig. 9). The development of a new band at 495 nm is considered to be due to the formation of an emissive exciplex between the acceptor CdS (h$^+$) and donor indole. Similar exciplex has been suggested to form between the CdS–TiO$_2$–indole system. However, its intensity under identical conditions was fairly low compared to the present system [12].

The illumination of reaction mixture containing Ag$^+$-activated composite catalyst CdS–TiO$_2$ and indole in the presence of O$_2$ by visible light ($\lambda_{ex} > 400$ nm) led to the production of bluish color product. Electronic and chromatographic study showed it to be the indigo similar to that observed with undoped CdS–TiO$_2$ system. The amount of indigo was measured by monitoring its absorption at 602 nm where the absorption due to indole does not interfere. The yield of indigo as a function of [Ag$^+$] added to CdS phase is shown in Fig. 10. At low [Ag$^+$] the amount of indigo increases linearly with the [Ag$^+$] up to 9.0×10^{-6} mol dm^{-3},

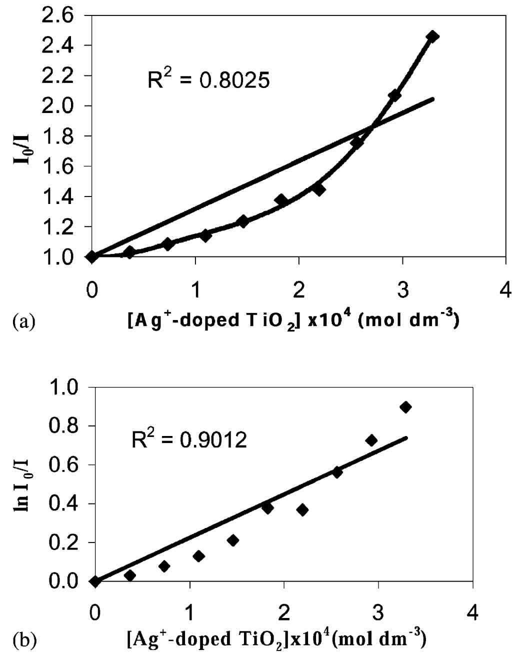

Fig. 6. (a) Stern–Volmer plot for the quenching of emission of $Cd(OH)_2$-coated Q-CdS in the presence of varying amount of Ag^+ (3.5×10^{-7} mol dm^{-3})-doped TiO_2 at 462 nm. (b) Perrin plot for the quenching of emission of $Cd(OH)_2$-coated Q-CdS in the presence of varying Ag^+ (3.5×10^{-7} mol dm^{-3})-doped TiO_2 at 462 nm.

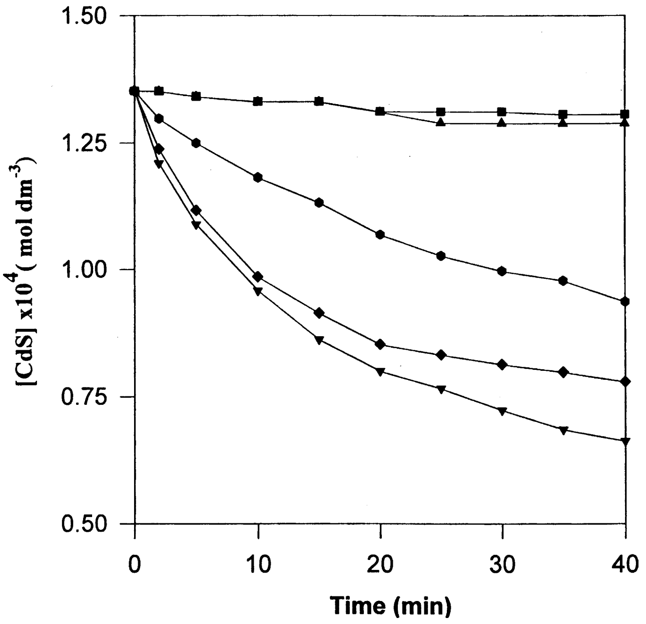

Fig. 7. Photodecomposition of CdS in $Cd(OH)_2$-coated Q-CdS (–■–); $Cd(OH)_2$-coated Q-CdS activated with Ag^+ (1.0×10^{-5} mol dm^{-3}) (–▲–); $Cd(OH)_2$-coated Q-CdS coupled with TiO_2 (1.28×10^{-3} mol dm^{-3}) (–●–); $Cd(OH)_2$-coated Q-CdS activated with Ag^+ (1.0×10^{-5} mol dm^{-3}) and coupled with TiO_2 (1.28×10^{-3} mol dm^{-3}) (–◆–); $Cd(OH)_2$-coated Q-CdS coupled with TiO_2 doped with Ag^+ (3.5×10^{-7} mol dm^{-3}) (–◀–) at pH = 11.0 at λ_{ex} = 400 nm.

thereafter, a further increase in the concentration of silver results in a decrease in the yield. At 9×10^{-6} mol dm^{-3} of Ag^+, ϕ_{indigo} was computed to be 0.14. This yield is about 75% higher compared to that of undoped CdS–TiO_2 catalyst under identical experimental conditions.

In an alternative plan TiO_2 was doped with silver and then these particles were coupled with $Cd(OH)_2$-coated Q-CdS. In reference to the quenching of bandgap emission in the absence of indole and the development of CT emission band (495 nm) in the presence of indole, the photophysics of these particles was very similar (Fig. 11) to that of observed when CdS was activated with silver and then coupled with TiO_2 (Fig. 9).

Fig. 12 presents a change in the yield of indigo as a function of silver added to the TiO_2 phase. At low [Ag^+] ($<3.5 \times 10^{-7}$ mol dm^{-3}) the amount of indigo increases almost proportionately. A further increase in the [Ag^+] causes a decrease in the yield of product. It follows the trend very

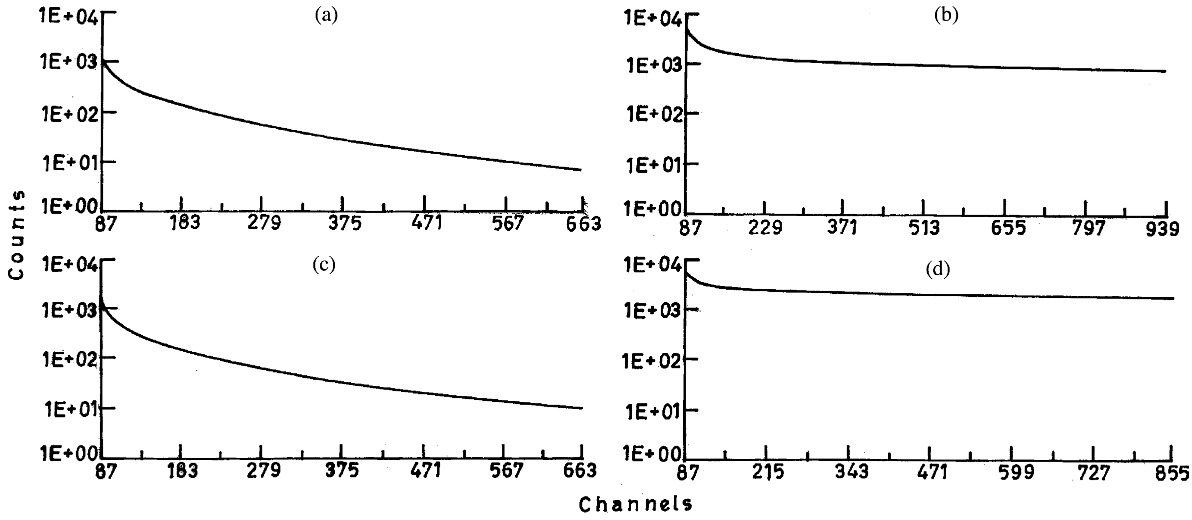

Fig. 8. Fluorescence decay curves of $Cd(OH)_2$-coated Q-CdS coupled with TiO_2 at 462 nm (a) and 650 nm (b); $Cd(OH)_2$-coated Q-CdS coupled with Ag^+ (3.5×10^{-7} mol dm^{-3})-doped TiO_2 at 462 nm (c) and 650 nm (d) at λ_{ex} = 375 nm. Time calibration: 5.079×10^{-11} s/channel.

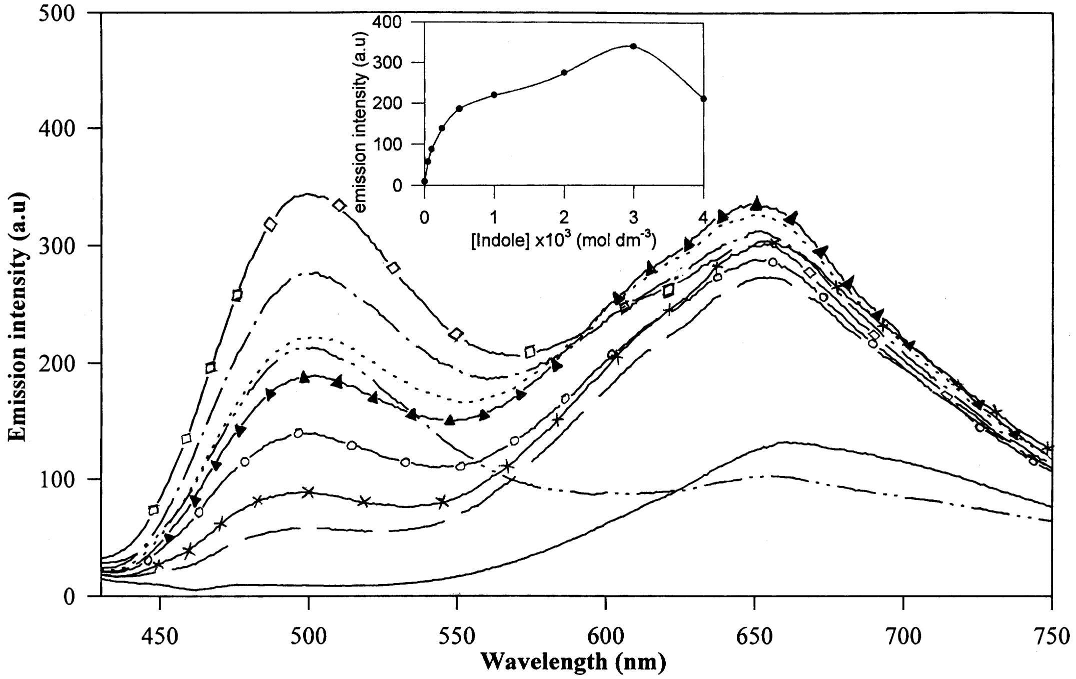

Fig. 9. Emission spectra of $Cd(OH)_2$-coated Q-CdS activated with Ag^+ (1.0×10^{-5} mol dm^{-3}) and coupled with TiO_2 (1.28×10^{-3} mol dm^{-3}) in the presence of different amounts of indole ($\times 10^{-3}$ mol dm^{-3}): 0.0 (—); 0.05 (- - -); 0.1 (–×–); 0.25 (–○–); 0.5 (–▲–); 1.0 (· · ·); 2.0 (– · –); 3.0 (–□–); 4.0 (– · · · –). Inset: variation of emission intensity vs. [indole] at 495 nm.

similar to that of intensity of exciplex emission as a function of [Ag^+] doped in TiO_2 (inset, Fig. 12). Obviously, both of these processes are related with the separation of charge. At 3.5×10^{-7} mol dm^{-3} of silver, ϕ_{indigo} was computed to be 0.16. This yield is exactly twofold higher than that of undoped TiO_2-coupled with CdS. Coupling of both TiO_2 and CdS, activated with the above-optimized amount of silver separately before coupling, did not enhance the yield of the product any further. At fairly high [Ag^+], a separate Ag_2S phase is formed which may also compete with indole for the interception of hole. The dynamics of charge carriers in this composite catalyst is illustrated in Fig. 13. Similar photocatalytic activity has been observed with other related additives and will be published elsewhere.

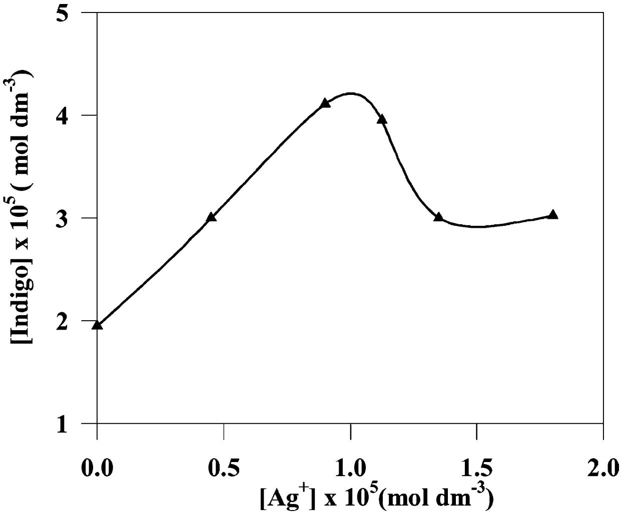

Fig. 10. Effect of activation of $Cd(OH)_2$-coated Q-CdS by adding Ag^+ on the yield of product obtained after 10 min of illumination [CdS] $= 1.35 \times 10^{-4}$ mol dm^{-3}, [TiO_2] $= 1.28 \times 10^{-3}$ mol dm^{-3} at pH $= 11.0$.

From the above observations it can be inferred that the initial separation of the charge in $Cd(OH)_2$-coated Q-CdS obtained by coupling with TiO_2 is essential for exhibiting the catalytic effect of Ag^+. The added silver ion modifies TiO_2 particles such that it traps more electrons on its surface (Eq. (3)) and these can now reside for longer period of time. It in turn serves to reduce the rate of e^-–h^+ recombination and enhances their reactivity with the redox couple.

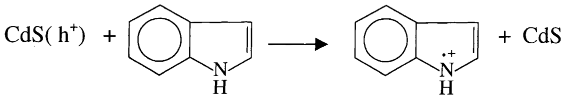

(6)

The negative effect at high [Ag^+] possibly arises due to the interception of hole by silver deposit which inhibits the reaction of h^+ with the substrate. The fact that the catalytic

$$CdS(h^+) + Ag \rightarrow Ag^+ + CdS \qquad (7)$$

effect with either TiO_2 doped with Ag^+ or CdS activated with Ag^+ are very much alike except that a little higher [Ag^+] is necessary for improving the charge separation with the latter system, it is likely that the Ag^+ which remains dissolved in CdS lattice creates additional trap sites in TiO_2 component similar to those in silver-doped TiO_2 catalyst

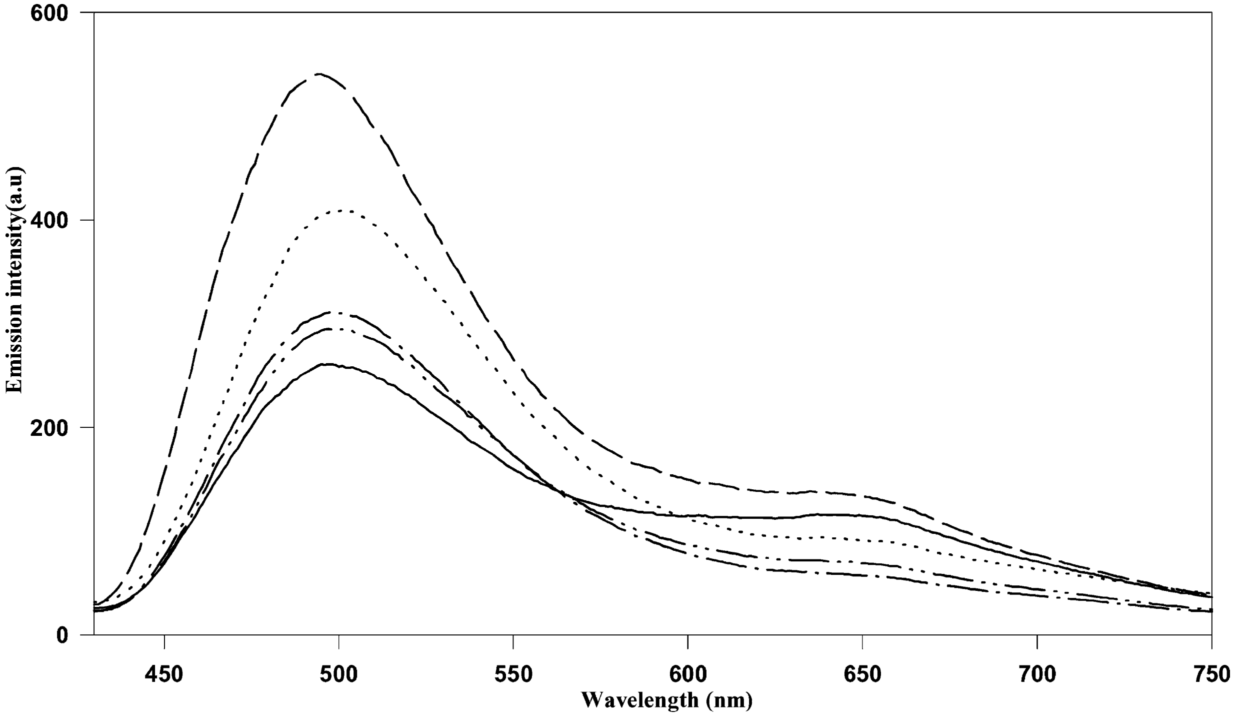

Fig. 11. Emission spectrum of Cd(OH)$_2$-coated Q-CdS coupled with TiO$_2$ containing different amount of Ag$^+$ ($\times 10^{-7}$ mol dm^{-3}): 0.87 (–···–); 1.75 (–·–); 3.5 (–––); 5.25 (···); 7.0 (—) in the presence of indole (3×10^{-3} mol dm^{-3}) at pH = 11.0.

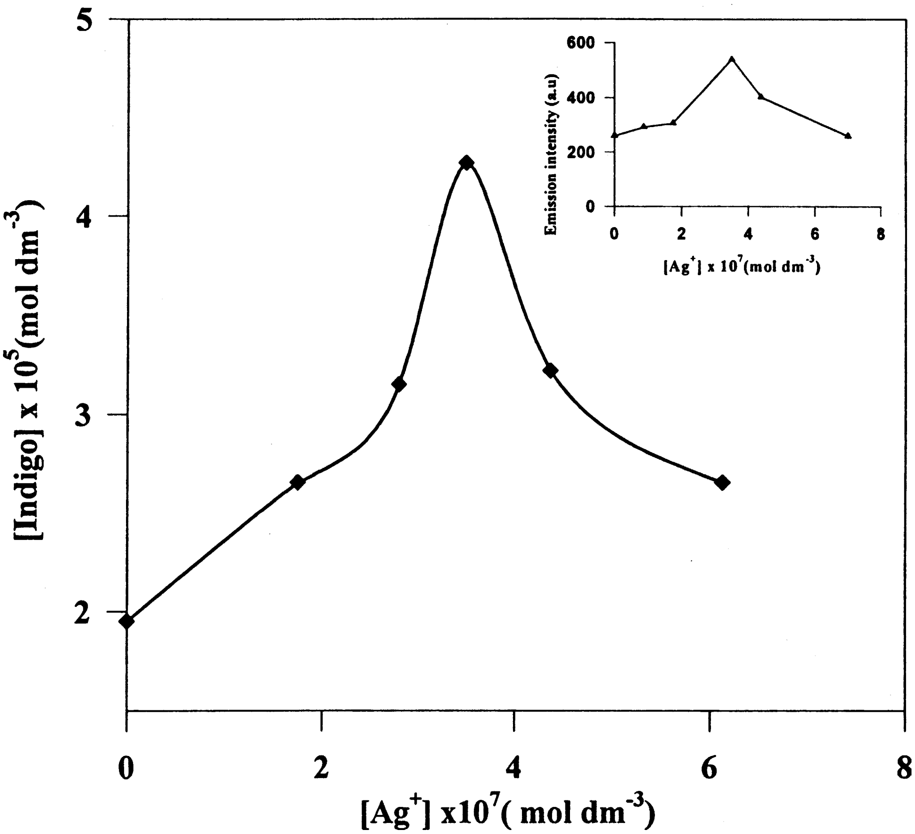

Fig. 12. Effect of doping of Ag$^+$ to colloidal TiO$_2$ on the yield of product obtained after 10 min of illumination [CdS] = 1.35×10^{-4} mol dm^{-3}, [TiO$_2$] = 1.28×10^{-3} mol dm^{-3} at pH = 11.0. Inset: variation of emission intensity of Cd(OH)$_2$-coated Q-CdS–TiO$_2$ in the presence of indole (3×10^{-3} mol dm^{-3}) as a function of [Ag$^+$] doped in TiO$_2$ at 495 nm.

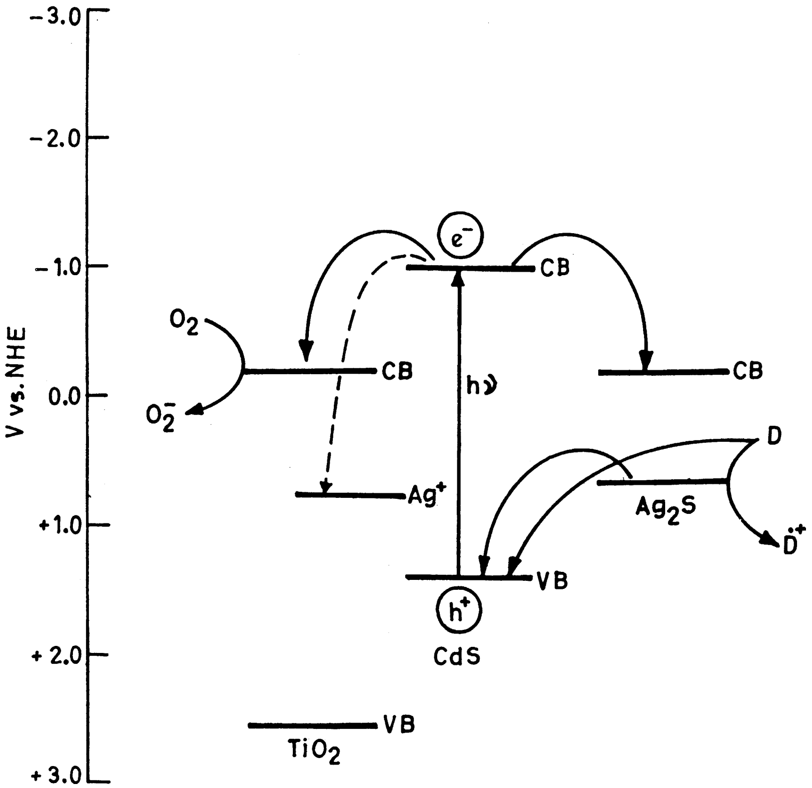

Fig. 13. Charge dynamics in Ag^+-activated coupled Q-CdS–TiO_2.

and the Ag_2S phase does not contribute significantly to the catalytic effect. This viewpoint is also supported by the experiments in which the coupling of both TiO_2 and CdS activated separately with the above-arrived optimum amount of Ag^+ did not affect the reaction efficiency.

An analysis of the relaxation of the charge carriers in CdS-Ag_2S and Ag^+-activated CdS–TiO_2 colloids reveal that in both cases there is a transport of shallowly trapped electron from the conduction band of CdS to the Ag^+ which increases the trapping of charge carriers in the deeper traps as was evidenced by decrease in $\langle\tau\rangle$ at 462 nm and increased $\langle\tau\rangle$ at 650 nm. However, the photocatalytic activity is seen to enhance enormously with the latter system. Obviously, the electron and hole could become available for reaction upon coupling of the two catalysts possibly by removing $Cd(OH)_2$ layer. The hydroxylation is known to reduce the conduction band potential of TiO_2 to a more negative value [29], which possibly facilitates this reaction effectively. A change in the electronic and emission spectra also illustrate a chemical interaction after coupling the two components (Figs. 4 and 5).

Some experiments were also designed by doping of TiO_2 colloids with Cu^{2+} and Mn^{2+} keeping rest of the components and conditions in this system identical as used above. The optimum concentration of Cu^{2+} was found to be 3.5×10^{-7} mol dm^{-3}. It enhanced the catalytic activity for oxidation of indole by about 40% compared to that of undoped catalyst. Mn^{2+} did not depict any catalytic action. These findings can be interpreted in terms of the redox potentials of Ag^+/Ag (0.76 V); Cu^{2+}/Cu (0.1 V) and Mn^{2+}/Mn (−1.029 V) couples. The photoelectron in the conduction band of TiO_2 is known to have a reduction potential of about −0.5 eV which can easily reduce Ag^+ and Cu^{2+} like metal ions and O_2 like species. In reference to the redox potentials of the used metal ions, the electron trapping would obviously be more efficient in case of TiO_2-doped with Ag^+ and the order of catalytic activity should be $Ag^+ > Cu^{2+} > Mn^{2+}$ which is indeed the case.

In summary, $Cd(OH)_2$-coated Q-CdS activated with Ag^+ is fairly photostable and sensitizes the reaction of indole–O_2 redox couple poorly. Coupling of Ag^+-containing $Cd(OH)_2$-coated Q-CdS with TiO_2 or Ag^+-doped TiO_2 with $Cd(OH)_2$-coated Q-CdS produces an efficient photocatalytic system. This photocatalyst is twice as effective compared to the non-activated composite CdS–TiO_2 system for performing synthetic photochemistry. A three component-coupled semiconductor (CdS–TiO_2–Ag_2S) is produced at higher [Ag^+]. Both the photophysics and the electron microscopy suggest the existence of these clusters. Pure Ag_2S phase does not participate in the observed photophysical changes and catalytic action. The composite semiconductors have lately been explored extensively for the development of efficient photocatalytic and photoelectrochemical solar conversion systems [30–32].

Acknowledgements

We gratefully acknowledge the generous financial assistance of Department of Science and Technology, New Delhi, to undertake this work. Thanks are also due to Prof. P. Natarajan, Director, NCUFP, Chennai and Director, AIIMS, New Delhi, for providing us the facilities of Single Photon Counter and TEM, respectively. AKJ thanks CSIR, New Delhi, for the award of SRF.

References

[1] A. Hagfeldt, M. Grätzel, Chem. Rev. 95 (1995) 49.
[2] M.R. Hoffmann, S.T. Martin, W. Choi, D.W. Bahnemann, Chem. Rev. 95 (1995) 69.
[3] M.A. Fox, M.T. Dulay, Chem. Rev. 93 (1993) 341.
[4] A. Henglein, Top. Curr. Chem. 143 (1988) 115.
[5] P.V. Kamat, Chem. Rev. 93 (1993) 267.
[6] H. Weller, Adv. Mater. 5 (1993) 88.
[7] D. Lawless, S. Kapoor, D. Meisel, J. Phys. Chem. 99 (1995) 10329.
[8] H. Fujii, M. Ohtaki, K. Eguchi, H. Arai, J. Mol. Catal. A: Chem. 129 (1998) 61.
[9] S. Hotchandani, P.V. Kamat, J. Phys. Chem. 96 (1992) 6834.
[10] K.R. Gopidas, M. Bohorquez, P.V. Kamat, J. Phys. Chem. 94 (1990) 6435.
[11] A. Henglein, H. Weller, A. Fojtik, M. Gutierrez, J. Jirkovsky, Ber. Bunsenges. Phys. Chem. 93 (1989) 593.
[12] A. Kumar, A.K. Jain, J. Mol. Catal. A: Chem. 165 (2001) 267.
[13] W. Choi, A. Termin, M.R. Hoffmann, Angew. Chem. Int. Ed. Engl. 33 (1994) 1091.
[14] J.-M. Herrmann, H. Tahiri, Y. Ait-Ichou, G. Lassaletta, A.R. Gonzalez-Elipe, A. Fernandez, Appl. Catal. B: Environ. 13 (1997) 219.
[15] A. Kumar, S. Kumar, Chem. Lett. (1996) 711.
[16] M.A. Poirier, G.T. Simley, Energy Sour. 8 (1985) 23.
[17] L. Spanhel, M. Haase, H. Weller, A. Henglein, J. Am. Chem. Soc. 109 (1987) 5649.
[18] J. Moser, M. Grätzel, J. Am. Chem. Soc. 105 (1983) 6547.
[19] D.R. James, Y.S. Liu, P. De Mayo, W.R. Ware, Chem. Phys. Lett. 120 (1985) 460.
[20] M. O'Neil, J. Marohn, G. McLendon, J. Phys. Chem. 94 (1990) 4356.
[21] H. Weller, Angew. Chem. Int. Ed. Engl. 32 (1993) 41.
[22] A. Kumar, D.P.S. Negi, J. Photochem. Photobiol. A: Chem. 134 (2000) 199.
[23] J.J. Ramsden, M. Grätzel, J. Chem. Soc., Faraday Trans. 1 80 (1984) 919.
[24] A. Kumar, S.. Kumar, J. Photochem. Photobiol. A: Chem. 83 (1994) 251.
[25] F.A. Cotton, G. Wilkinson, Advanced Inorganic Chemistry, 5th ed., 1988, p. 605.
[26] R.C. Weast (Ed.), CRC Handbook of Chemistry and Physics, CRC Press, Ohio, 1977, p. B254.
[27] J.F. Reber, M. Rusek, J. Phys. Chem. 90 (1986) 824.
[28] L. Spanhel, H. Weller, A. Fojtik, A. Henglein, Ber. Bunsenges. Phys. Chem. 91 (1987) 88.
[29] D. Duonghong, J. Ramsden, M. Grätzel, J. Am. Chem. Soc. 104 (1982) 2977.
[30] C. Nasr, S. Hotchandani, W.Y. Kim, R.H. Schmehl, P.V. Kamat, J. Phys. Chem. B. 101 (1997) 7480.
[31] I. Bedja, P.V. Kamat, J. Phys. Chem. 99 (1995) 9182.
[32] R. Vogel, K. Pohl, H. Weller, Chem. Phys. Lett. 174 (1990) 241.